Model-Based Probabilistic Collision Detection in Autonomous Driving

Matthias Althoff, Olaf Stursberg, *Member, IEEE*, and Martin Buss, *Member, IEEE*

Abstract—The safety of the planned paths of autonomous cars with respect to the movement of other traffic participants is considered. Therefore, the stochastic occupancy of the road by other vehicles is predicted. The prediction considers uncertainties originating from the measurements and the possible behaviors of other traffic participants. In addition, the interaction of traffic participants, as well as the limitation of driving maneuvers due to the road geometry, is considered. The result of the presented approach is the probability of a crash for a specific trajectory of the autonomous car. The presented approach is efficient as most of the intensive computations are performed offline, which results in a lean online algorithm for real-time application.

Index Terms—Autonomous cars, behavior prediction, interaction, Markov chains, reachable sets, safety assessment, threat level, uncertain models.

I. INTRODUCTION

OVER THE PAST few years, new driver-assistant systems have successfully emerged on the market as they compensate the shortcomings of human drivers, such as inevitable reaction times for emergency brakes or deficiencies in vehicle stabilization. However, the cognitive capabilities of humans are excellent and valuable in unexpected driving situations as well as for the correct interpretation of a traffic situation. Consequently, the next step toward intelligent vehicles is the implementation of basic cognitive capabilities as it has been tried in many research projects, among them the collaborative research center *Cognitive Automobiles* [29], in which this paper has been carried out.

One of the human abilities in traffic is the estimation of the threat level of planned actions. Maneuvers such as overtaking, lane changing, or intersection crossing are mainly evaluated according to a ratio of risk and time efficiency. As the consequences of a started maneuver affect the future development of a traffic situation, prediction is inevitable to assess the danger of the taken action. In this paper, a technical realization for the safety assessment of the driving maneuvers of autonomous cars is proposed, which is based on the prediction of traffic situations. In contrast to predictive approaches, nonpredictive methods are based on the record and evaluation of traffic situations that have resulted in dangerous situations; see, e.g., [1].

M. Althoff and M. Buss are with the Institute of Automatic Control Engineering (LSR), Technische Universität München, 80290 München, Germany (e-mail: althoff@tum.de; mb@tum.de).

O. Stursberg is with the Institute of Control and System Theory, University of Kassel, 34121 Kassel, Germany (e-mail: stursberg@uni-kassel.de).

Behavior prediction of human drivers has widely been investigated, e.g., in [21], [25], and [33]. As reported in the literature, human driver prediction within the *ego vehicle* (i.e., the vehicle for which the safety assessment is performed) can be conducted with the help of learning mechanisms such as neural networks or filter techniques, as, e.g., Kalman filters. The same approaches can be applied for the traffic scenes that are observed from a fixed location, such as intersections, which allows typical behavior patterns of the specific scene to be learned; see, e.g., [17] and [30].

Another possibility to predict traffic situations is to simulate single behaviors of traffic participants [10], [15], which results in measures like *time to collision* or *predicted minimum distance*. Due to the efficiency of single simulations, these approaches are already widely implemented in cars. However, single simulations do not consider uncertainties in the measurements and actions of other traffic participants, which may lead to unsatisfying collision predictions [20]. A more sophisticated threat assessment considers multiple simulations of other vehicles considering different initial states and changes in their inputs (steering angle and acceleration). These so-called Monte Carlo methods have been studied in [11], [12], and [14].

Another method to investigate the possible behaviors of traffic participants is reachability analysis; see, e.g., [3], [7], and [9]. For a given set of initial states and disturbance values, a reachable set contains all the possible states that the system trajectories can evolve into. If, for a traffic scenario, the reachable positions of the ego vehicle do not intersect the reachable positions of another vehicle, then these vehicles cannot crash. Reachable sets for vehicles have been investigated in [27] and [31]. It has been shown that the planned paths of autonomous vehicles are too often evaluated as unsafe by this method, because the reachable sets of other vehicles rapidly cover all positions the autonomous vehicle could possibly move to. For this reason, the reachable sets are enhanced by stochastic information to the so-called *stochastic reachable sets* in previous papers of the authors [2], [4], [6]. The stochastic information allows not only the checking of whether a planned path of the ego vehicle may result in a crash but also with which probability. Consequently, the possible driving strategies of autonomous cars can be evaluated according to their safety. Stochastic reachable sets have also been investigated for air traffic safety [16] and fault diagnosis [23], [28].

It is further emphasized that traffic prediction has to consider the interaction between vehicles. The interaction between vehicles has widely been studied in microscopic traffic simulations [24] and within Monte Carlo techniques [11], [12], [14]. The problem one faces with interaction is that the simulations result
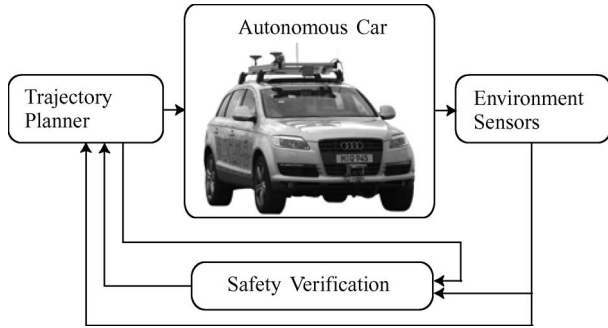
Fig. 1. Conception of safety assessment.

Fig. 2. Stochastic reachable sets of traffic participants.

Fig. 3. Repetitive computation of reachable sets.

in a fast-growing tree of possible situations to be considered. If only discrete actions (e.g., lane change) at discrete points of time are taken into account, then the computational complexity is $O(\mu^{\rho \cdot \nu})$, where μ is the number of possible actions, ρ is the number of time steps of the prediction, and ν is the number of traffic participants (see [13]). This worst-case complexity, however, can be reduced by discarding impossible or unrealistic behaviors. The consideration of interaction also causes additional complexity for the computation of stochastic reachable sets; however, the incorporated interaction mechanism of the presented approach is efficient in the sense that the computations can be applied online using a desktop PC.

II. MOTIVATION AND PROBLEM STATEMENT

Clearly, autonomous driving requires a control loop that contains a perception and a planner module (see Fig. 1). The perception module detects traffic situations and extracts relevant information, such as the road geometry as well as static and dynamic obstacles. To fulfill the driving task, the planner module computes the trajectories that the autonomous car is tracking with the use of low-level controllers. A major constraint for the trajectory planner is that the generated trajectories have to be safe, i.e., no static and dynamic obstacles must be hit. The task of circumventing static obstacles can be ensured by checking whether the static obstacle intersects with the vehicle body of the autonomous car following the planned path. For dynamic obstacles, the safety assessment is much more intricate as their future actions are unknown. For this reason, sets of possible behaviors of other traffic participants are considered, which are checked with the planned path of the autonomous car in a dedicated safety verification module (see Fig. 1). Paths that fulfill the safety requirements are executed and conservatively replanned otherwise, e.g., by braking the car.

The safety verification module that is described in this paper requires the description of a traffic situation containing the following information gathered by the perception module:

1) the planned trajectory of the autonomous car;
2) the geometric description of the relevant road sections;
3) the position and geometry of static obstacles;
4) the position, velocity, and classification of dynamic obstacles.

Static obstacles are a special case of dynamic obstacles with zero velocity, and for that reason, the discussion is con-
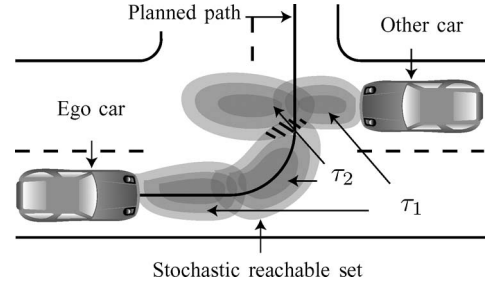
tinued for dynamic obstacles only. The classification groups the dynamic obstacles ($\hat{=}$ traffic participants) into *cars*, *trucks*, *motorbikes*, *bicycles*, and *pedestrians*. As the measurement of positions and velocities of the other traffic participants is uncertain, the presented approach allows the measured data to be specified by a probability distribution. However, the minimum requirement is that all relevant traffic participants are detected at all. The region where the probability density is nonzero is referred to as the initial set. Given this set, the future set of positions possibly occupied by the traffic participant is denoted as the *reachable set*. Analogously, given the initial probability distribution of a traffic participant, the future probability distribution is also referred to as the *stochastic reachable set*.
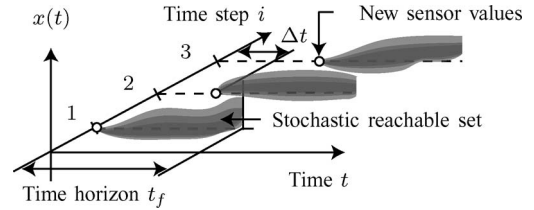
Reachable sets of other traffic participants allow to guarantee the safety of the planned trajectory for a prediction horizon t_f if they do not intersect the reachable set of the ego car within the specified horizon. For the case of a possible crash, the probability distribution within the reachable set is used to determine the probability of the crash. This is illustrated in Fig. 2, where stochastic reachable sets are shown for the time intervals $\tau_1 = [0, t_1]$ and $\tau_2 = [t_1, t_2]$ (dark color indicates high probability density). Within the time interval τ_1, a crash between both cars is impossible, whereas for the second time interval τ_2, the crash probability is nonzero. It is obvious that the computation of the crash probability has to be faster than real time for online application. To update the crash probability prediction after a time interval Δt based on new sensor values, its computation has to be faster than real time by a factor of $t_f/\Delta t$. This is illustrated in Fig. 3 for the reachable set of a single variable $x(t)$.

III. MODELING OF TRAFFIC PARTICIPANTS

This paper focuses on the safety assessment of autonomous cars driving on a road network, i.e., the motion of traffic participants is constrained along designated roads. On that account, the possible paths of traffic participants are determined by the finite set of decisions {*left turn*, *right turn*, *go straight*}.
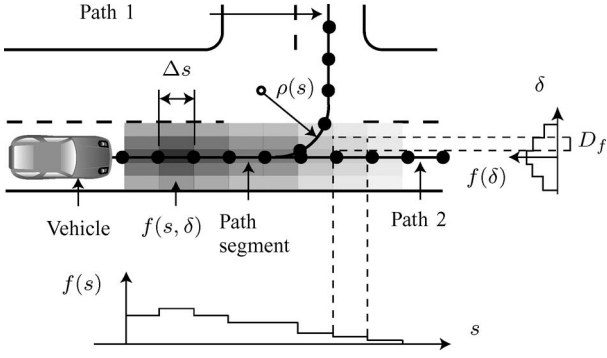
Fig. 4. Probability distribution of the position of a vehicle along a path-aligned coordinate system.

Fig. 5. Probability distribution of the vehicle center and the vehicle body.

The extension to multilane roads with the additional actions {*left lane change*, *right lane change*} is the subject of future work. The deviation along these major paths is modeled by a piecewise constant probability density function $f(\delta)$, where δ is the lateral deviation from a driving path. The possible driving paths of a road network section, as well as the deviation probability distribution $f(\delta)$, are shown in Fig. 4. The deviation probability can be adjusted to different classes of traffic participants: Bicycle drivers are more likely to be found close to the curb, whereas cars and trucks are driving more likely in the center of a lane. For unstructured environments, such as parking spaces or pedestrians on a square, the motion of vehicles/people cannot be described along paths. For these kinds of scenarios, the approach presented in [26] is suggested, which uses the same mathematical principles as presented in this paper.

The longitudinal probability distribution of the position of the vehicles is obtained by a dynamic model. After denoting the position of the volumetric center of the vehicles along a path with s, the velocity with v, and the absolute acceleration with a, the longitudinal dynamics for the driving input u can be described as

$$\dot{s} = v \qquad \dot{v} = \begin{cases} c_1 \cdot \left(1 - (v/c_2)^2\right) \cdot u, & u > 0 \\ c_1 \cdot u, & u \leq 0 \\ 0, & v \leq 0 \end{cases} \qquad (1)$$

subject to the constraint

$$a \leq \bar{a}^{\max} \qquad (2)$$

where $a = \sqrt{a_N^2 + a_T^2}$, $a_N = v^2/\rho(s)$, and $a_T = \dot{v}$. The constant c_1 models the maximum possible acceleration due to tire friction, and c_2 models the top speed—these constants are chosen according to the specific properties of the different classes of traffic participants. The acceleration input varies from $[-1, 1]$, where -1 represents full braking, and 1 represents full acceleration. Backward driving on a lane is not considered [see (1) $(\dot{v} = 0, v \leq 0)$]. The function $\rho(s)$ maps the path coordinate s to the radius of curvature of the path, and a_N and a_T are the normal and tangential accelerations, respectively. The constraint in (2) models that the tire friction of a vehicle only allows a limited absolute acceleration $\bar{a}^{\max}$ (Kamm's circle). In the case in which a traffic participant is violating
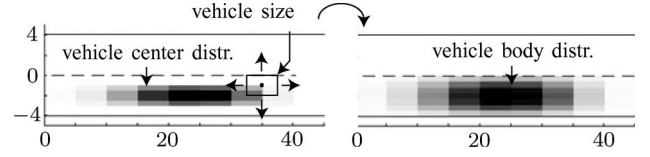
the traffic regulations, such as driving on the wrong lane, the approach for unstructured motion in [26] is applied for this specific traffic participant. The dynamic equations in (1) are exemplarily chosen and can easily be exchanged against a different set of equations. Based on the dynamics specification, the longitudinal probability distribution $f(s)$ is obtained. Assuming that the lateral distribution is independent from the longitudinal distribution, the overall probability distribution is computed as $f(s, \delta) = f(s) \cdot f(\delta)$ (see also Fig. 4). Thus, the probability distribution is described in a curved path-aligned coordinate system, as also used in, e.g., [14].

It is emphasized that the lateral and longitudinal distributions $f(\delta)$ and $f(s)$ refer to the volumetric center of the vehicles. However, for visualization reasons, all the figures in this paper show the vehicle body density that is taking the vehicle size into account (see Fig. 5).

IV. REACHABLE SETS OF TRAFFIC PARTICIPANTS

This section deals with the computation of reachable sets for traffic participants (no stochastic information). Given the dynamics of a traffic participant as $\dot{x} = f^{TP}(x(t), u(t))$, where $x \in \mathbb{R}^n$ is the state, and $u \in U \subset \mathbb{R}^m$ is a Lipschitz continuous input constrained by the set U, the exact reachable set $R^e(r)$ at time $t = r$ can be defined as

$$R^e(r) = \left\{ x(r) | x(r) = x(0) + \int_0^r f^{TP}\left(x(\tau), u(\tau)\right) d\tau \right.$$
$$\left. x(0) \in X_0, u(\tau) \in U \right\}.$$

In general, the exact reachable set of a system cannot be computed [19]. However, one can always compute an over-approximation, which is denoted as $R(r) \supseteq R^e(r)$. The over-approximated reachable set for a time interval is defined as $R([0, r]) := \bigcup_{t \in [0, r]} R(t)$.

In this paper, overapproximations of reachable sets of non-linear dynamic systems are computed as presented in [5]. An example of the overapproximated reachable set of (1) for $u \in [0.5, 1]$ and $t \in [0, 2]$ s is given in Fig. 6 for two different initial sets. Additionally, sample trajectories starting from the initial set are shown, where the states at times $k \cdot \Delta t^*$, $k = 0, \ldots, 4$, $\Delta t^* = 0.5$ s are marked by a circle. If one is only interested in the reachable interval of the position and velocity of a vehicle driving along a straight path, then the following special case can be formulated.

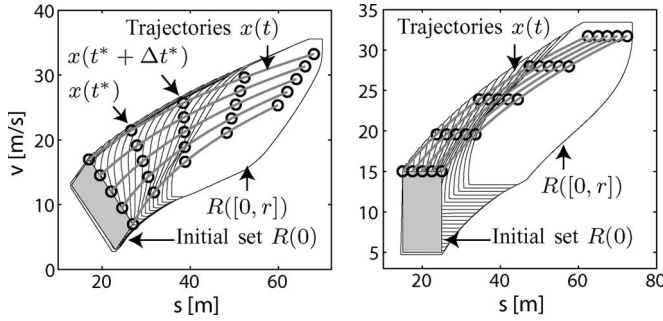*Proposition 1:* Given a vehicle driving along a straight path with dynamics subject to (1) and the initial condition

Fig. 6.   Reachable sets of a vehicle for different initial sets.

$x(0) \in X(0) = S(0) \times V(0)$, where $S(0) = [\underline{s}(0), \overline{s}(0)]$ and $V(0) = [\underline{v}(0), \overline{v}(0)]$ are the position and velocity intervals, respectively. The reachable 2-D interval $X(t) = [\underline{x}(t), \overline{x}(t)]$ of position and velocity is given by

$$\underline{x}(t) = \underline{x}(0) + \int_0^t f^{TP}(x(\tau), u(\tau))\, d\tau, \qquad u(\tau) = -1$$

$$\overline{x}(t) = \overline{x}(0) + \int_0^t f^{TP}(x(\tau), u(\tau))\, d\tau, \qquad u(\tau) = 1.$$

The proof is omitted, as it is clear that the greatest position and velocity are reached when the vehicle starts with the greatest initial position and velocity within the initial set under full acceleration. The analogous argumentation holds for the lowest position and velocity. Note that this argumentation is only applicable if there exists an initial state that jointly contains the maximum initial position and velocity. This is always the case when the initial set is a 2-D interval, which is in contrast with the left example in Fig. 6, for which proposition 1 is not applicable. In the left example, the maximum reachable position at different times is reached from trajectories starting from different initial states. However, if one is only interested in the reachable position, and the initial set is a 2-D interval, as shown in the right example of Fig. 6, the result of Proposition 1 gives the exact reachable interval of the position coordinate.

For the case of a curved path, one has to consider the tire friction constraint in (2). For a given radius profile $\rho(s)$, the minimum and maximum admissible inputs $\underline{u}(s)$ and $\overline{u}(s)$ can be obtained as presented, e.g., in [32]. By changing $u(\tau) = -1$ to $u(\tau) = \underline{u}(s(\tau))$ and $u(\tau) = 1$ to $u(\tau) = \overline{u}(s(\tau))$ in Proposition 1, one can compute the reachable positions for a curved road. The speed limits on a road can be handled by cutting off the previously computed speed profile $v(s)$ at $v^{\max}$ by assigning $\overline{u}(s) = 0$ if $v(s) > v^{\max}$.

V. STOCHASTIC REACHABLE SETS OF TRAFFIC PARTICIPANTS

As stated in the previous section, the exact computation of reachable sets is only possible for a limited class of systems [19]. Hence, it is obvious that for the more general problem of stochastic reachable sets, one has to apply (conservative) approximation techniques as well. One of the most frequently used techniques is to approximate stochastic processes by Markov chains. The techniques for the abstraction to Markov chains are manifold, where many of them couple the time interval between the updates of the probability distribution with the accuracy of the abstraction, see, e.g., [16] and [18]. However, this coupling is unfavorable in terms of real-time applicability, as a required approximation accuracy may lead to short update times of the probabilities and consequently to too many update iterations that cannot be handled in real time. For this reason, the update intervals and the approximation accuracy is decoupled, as in [22] and [28]. The presented abstraction method for nonlinear systems with unknown inputs is conservative, which means that the reachable set of the Markov chain is an overapproximation of the reachable set of the original stochastic process. Note that, in contrast to the reachable set, the probability distribution is an approximation, as in case of an overapproximation, its integral would be greater than one and thus destroys an axiom of the probability calculus.

The abstraction of the continuous dynamics of the traffic participants to Markov chains is computed offline. During the online execution of the algorithm, for each traffic participant, a Markov chain is instantiated. The interaction between traffic participants is established by influencing the acceleration probabilities of traffic participants by the state (position, velocity) and the acceleration of other traffic participants. This means that the traffic participants of a traffic situation are not combined in a single Markov chain, but represented by separate Markov chains. Thus, the complexity of the algorithm is N times the worst-case complexity of the computation of a single traffic participant, and N is the number of considered traffic participants.

It is also emphasized that the abstraction to Markov chains discussed from Sections V-A–D is only performed for other vehicles, as the motion of the ego vehicle is planned within the vehicle and thus known. The ego vehicle is separately discussed in Section V-E.

A. Abstraction by Markov Chains

A Markov chain is a stochastic dynamic system with discrete states $z \in \mathbb{N}^+$. There are discrete- and continuous-time Markov chains. In this paper, discrete-time Markov chains are used, such that $t \in \{t_1, t_2, \ldots, t_f\}$, where t_f is the prediction horizon, and $t_{k+1} - t_k = T \in \mathbb{R}^+$ is the time step increment. In Markov chains, the current state is not exactly known, but probabilities $p_i = P(z = i)$ describe that the system is in state $z = i$, which leads to a probability vector p. By definition, the probability vector for the next time step t_{k+1} is a linear combination of the probability vector of the previous time step t_k, i.e.,

$$p(t_{k+1}) = \Phi \cdot p(t_k) \tag{3}$$

where Φ is referred to as the transition matrix. The generation of a Markov chain model can be divided into two steps: First, the state space of the original continuous system is discretized into cells representing the discrete states. Second, the transition probabilities from one cell to another cell have to be determined, which are stored in the transition matrix of the Markov chain.
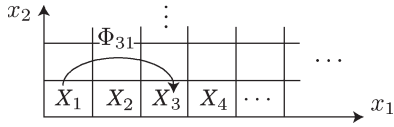
Fig. 7. Discretization of the state space.

1) Discretization of the State and Input Space: In this paper, a region $X \subset \mathbb{R}^2$ of the continuous state space of (1) is discretized in orthogonal cells of equal size, which results in rectangular cells with the coordinates $x_1 := s$ and $x_2 := v$ (see Fig. 7). This discretization allows describing the cells X_i (with index i referring to the represented discrete state) by the 2-D interval $X_i =]\underline{x}_i, \overline{x}_i]$, $\underline{x}_i, \overline{x}_i \in \mathbb{R}^2$, and $X = \bigcup X_i$. In an analogous way, a region $U \subset \mathbb{R}$ of the input space of (1) is discretized into intervals U^α such that $U = \bigcup U^\alpha$. The index α refers to the value of the discrete input, which is denoted by y. To distinguish between indexes referring to states or inputs, state indexes are subscripted and in Latin, whereas the input indexes are superscripted and in Greek.

2) Transition Probabilities of the Markov Chain: The transition probabilities store the probabilities that the system state changes from i to j: $\Phi_{ji} = P(z(t_{k+1}) = j | z(t_k) = i)$. In this paper, the transition probabilities depend on the discrete input α as well. For this reason, a different transition probability matrix Φ^α is computed for each discrete input α. The value of a transition probability Φ_{ji}^α is obtained by the reachable set $R_{ji}^\alpha(T)$ starting from $x(0) \in X_i$ under the effect of the input $u \in U^\alpha$, where the cells X_i and U^α represent the corresponding discrete state and input of Φ_{ji}^α. Note that the time T of the reachable set is equal to the time step increment T of the Markov chain. The probability of reaching cell j is computed as the volumetric fraction of the reachable set intersecting with the cell X_j, i.e.,

$$\Phi_{ji}^\alpha(T) = \frac{V(R_i^\alpha(T) \cap X_j)}{V(R_i^\alpha(T))} \quad (4)$$

where $V()$ is an operator returning the volume. As soon as a cell is reached by $R_i^\alpha(T)$, the probability that the cell can be reached is nonzero. As only the probability of reaching a cell is stored, the information is lost to which part of the cell can be reached. For this reason, the reachable cells (cells with nonzero probability) of the Markov chain overapproximate each corresponding reachable set $R_i^\alpha(T)$. The probability values itself are approximative (in contrast to overapproximative reachable sets) as an equal distribution of the system state within the reachable sets is assumed in (4).

In an analogous way, one can compute the transition probabilities $\Phi_{ji}^\alpha([0, T])$ for $t \in [0, T]$ by substituting $R_i^\alpha(T)$ with $R_i^\alpha([0, T])$, which is the reachable set for $t \in [0, T]$. Due to computational reasons [5], the reachable set $R_i^\alpha([0, T])$ is obtained from $\bigcup_{l=0}^{T/r-1} R_i^\alpha([l \cdot r, (l+1) \cdot r])$, where T is a multiple of r such that

$$\Phi_{ji}^\alpha([0, T]) = \frac{r}{T} \sum_{l=0}^{T/r-1} \Phi_{ji}^\alpha([l \cdot r, (l+1) \cdot r]).$$
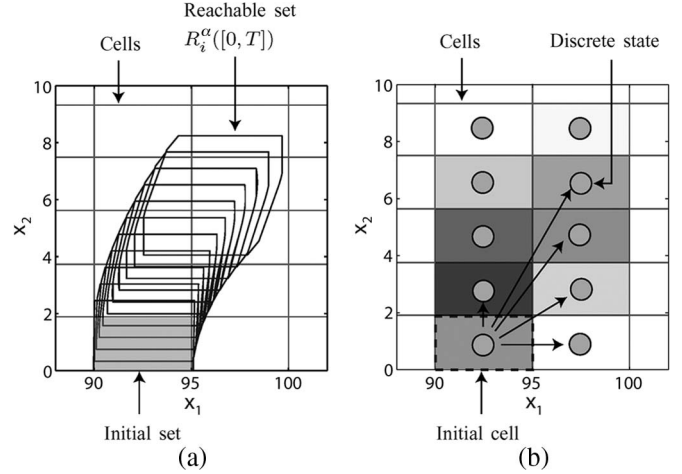

Fig. 8. Reachable set of the original system and the corresponding stochastic reachable set of the abstracting Markov chain. (a) Reachable set for a time interval. (b) Reachable cells for a time interval.

Note that the transition probabilities in $\Phi_{ji}^\alpha(T)$ and $\Phi_{ji}^\alpha([0, T])$ are computed offline such that computationally expensive operations are performed beforehand. The reachable set of $R_i^\alpha([0, T])$ is exemplarily shown for the case of $T/r = 10$ in Fig. 8(a). The corresponding stochastic reachable set, which results from $\Phi_{ji}^\alpha([0, T]) \cdot p(0)$ with $p_m(0) = 0$ for $m \neq i$ and $p_i(0) = 1$ ($i \doteq$ Initial cell), is illustrated in Fig. 8(b). The circles symbolize the discrete states, which are assigned to the corresponding cells. A transition to a cell is the more likely that the darker the color of the cell is.

B. Computing Stochastic Reachable Sets Using Markov Chains

After the discretization of the state space, the stochastic reachable set can fully be described by the probability vector p of the Markov chain. For a single Markov chain, the evolution of the probability vector can be computed as in (3). However, in this paper, Markov chains for different discrete inputs α as well as for the time point and time interval solution are computed. Hence, (3) has to be extended. The first extension is that the probability distribution within a time interval is computed based on the distribution at a time point (for a given input α). Thus, the probability distribution at certain time points serves as a support for the time interval computations

$$p(t_{k+1}) = \Phi^\alpha(T) \cdot p(t_k)$$
$$p([t_k, t_{k+1}]) = \Phi^\alpha([0, T]) \cdot p(t_k). \quad (5)$$

This is justified by the fact that the transition probability matrix $\Phi^\alpha([0, T])$ is also computed based on the initial cell at the beginning of the considered time interval. Note that the indexes of the matrix Φ^α and the vector $p(t_k)$ are neglected, as is commonly done in linear algebra. In (5), the input α is known and globally applied to all states i of the Markov chain. For the next extension, the conditional probability $q_i^\alpha = P(y = \alpha | z = i)$ is defined. The joint probability of the state and input
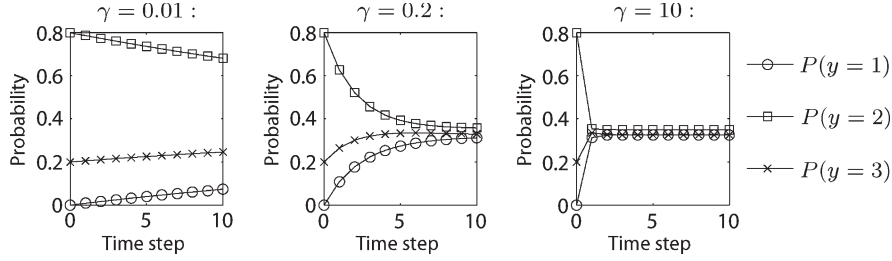
Fig. 9.   Input evolution for $\gamma = 0.01, 0.2,$ and 10.

is abbreviated as $p_i^\alpha := P(z = i, y = \alpha) = P(y = \alpha | z = i) \cdot P(z = i) = q_i^\alpha \cdot p_i$. It is also clear that $p_i = \sum_\alpha p_i^\alpha$, where $\sum_\alpha$ denotes the sum over all possible values of α. As a novelty compared to earlier work in [6], the probability distribution of the input is dynamically changed by another Markov chain with transition matrix Γ_i, depending on the system state i. This allows a more accurate modeling of driver behavior by considering how frequently and how intense the acceleration command is changed. The input probability distribution instantly changes at discrete times t_k, which is indicated by a prime, i.e.,

$$q_i^\beta(t_k)' = \Gamma_i^{\beta\alpha} \cdot q_i^\alpha(t_k) \rightarrow p_i^\beta(t_k)' = \Gamma_i^{\beta\alpha} \cdot p_i^\alpha(t_k). \quad (6)$$

The mapping has to be performed for each discrete state value $z = i$, unless $p_i^\alpha = 0 \; \forall\alpha$. For a better distinction to Φ, the indexes of Γ describing the input transitions are superscripted—as also done for the input indexes of the probability p. The introduction of the joint probability p_i^α requires a slight modification of (5), where the joint probabilities p_i^α have to be updated for each input value α instead of only a single input value, i.e.,

$$p^\alpha(t_{k+1}) = \Phi^\alpha(T) \cdot p^\alpha(t_k)$$
$$p^\alpha([t_k, t_{k+1}]) = \Phi^\alpha([0, T]) \cdot p^\alpha(t_k).$$

In contrast to the computation of the transition matrices Φ^α for the states, the transition matrices Γ_i for the inputs cannot be computed based on a dynamic model. This is because the input/driving commands to other vehicles are provided by humans or complex computer systems (when vehicles will drive autonomously in the future) for which the system dynamics is unknown. As a consequence, the transition matrices Γ_i have to be learned by observation or set by a combination of simulations and heuristics, where the latter is used in this paper. The input transition matrix is composed of an input dynamics matrix Ψ and a priority vector λ, where the prioritization results from many aspects, such as speed limits or interaction with other vehicles. The input dynamics matrix Ψ and the priority vector λ are combined into the following:

$$\Gamma_i^{\beta\alpha} = \text{norm}\left(\hat{\Gamma}_i^{\beta\alpha}\right) := \frac{\hat{\Gamma}_i^{\beta\alpha}}{\sum_\beta \hat{\Gamma}_i^{\beta\alpha}}$$

$$\hat{\Gamma}_i^{\beta\alpha} = \text{diag}\left(\lambda_i^\beta\right) \cdot \Psi^{\beta\alpha} \qquad \forall i : \sum_\beta \lambda_i^\beta = 1, \quad 0 \le \lambda_i^\beta \le 1.$$

(7)

The intermediate result $\hat{\Gamma}_i^{\beta\alpha}$ is normalized by the sums of the columns such that they are summing up to 1 to ensure that the sum of the probability vector stays 1 after the multiplication with Γ [see (6)]. The state dependence is modeled by the priority vector λ, whereas the input dynamic matrix Ψ is independent of the state. The foregoing formula has the following special cases.

1) $\lambda_i^\beta = 0$: Regardless of the input dynamics matrix Ψ, the input β of state i is prohibited $(q_i^\beta = 0)$ as the corresponding row of Γ becomes 0.
2) $\lambda_i^\beta = (1/\kappa) \quad \forall i, \beta$ (κ is the number of inputs): No input is prioritized such that $\Gamma_i = \Psi$.
3) $\Psi = I$ (I is the identity matrix): $\Gamma_i = I$, regardless of λ, such that the input probability is unchanged.
4) $\Psi = (1/\kappa)O(O$ is a matrix of ones): The multiplication $\Gamma_i \cdot q_i$ results in $\text{norm}(\text{diag}(\lambda_i)(1/\kappa)O) \cdot q_i = \lambda_i$. Thus, a certain input probability distribution $q_i = \lambda_i$ is enforced regardless of the probability distribution of the previous time step.

To separately discuss the effect of Ψ, λ is set to $\lambda_i^\beta = (1/\kappa) \quad \forall i, \beta$, such that $\Gamma_i = \Psi$, and therefore, the input dynamics matrix Ψ specifies with which probability the input is changed from input α to input β [see (6)]. These transition probabilities are set according to the heuristics that the bigger the change of the input,[1] the more unlikely is this change. A transition matrix that considers this aspect and further contains the special cases of $\Psi = I$ and $\Psi = (1/\kappa)O$ is

$$\Psi^{\beta\alpha}(\gamma) = \text{norm}\left(\hat{\Psi}^{\beta\alpha}(\gamma)\right), \qquad \hat{\Psi}^{\beta\alpha}(\gamma) = \frac{1}{(\beta - \alpha)^2 + \gamma}.$$

The parameter γ allows the gradual interpolation of the extreme cases $\Psi = I$ and $\Psi = (1/\kappa)O$, which are represented by the limit $\lim_{\gamma \to 0} \Psi(\gamma) = I$ and the other limit $\lim_{\gamma \to \infty} \Psi(\gamma) = (1/\kappa)O$. Informally speaking, a low value of γ models drivers that do not change their input often, whereas a high value models drivers that change their input often. The higher the value of γ, the faster the initial input probability distribution converges to a steady-state distribution, which can be changed by the priority vector λ. This is illustrated in Fig. 9 for three inputs, where the high input numbers represent high positive

---

[1]As the discrete inputs are numbered in increasing order according to the acceleration intervals, the difference between the input numbers is a measure for the change of the acceleration interval.
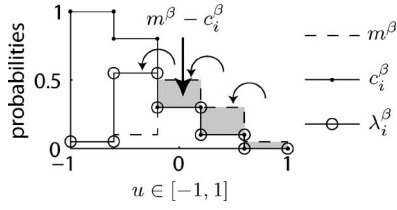
Fig. 10.   Combining a probability distribution with a probabilistic constraint.

acceleration, such that the first input $y = 1$ represents full braking, and the last input $y = 3$ represents full acceleration. The initial probabilities are set to $P(y = 1) = 0$, $P(y = 2) = 0.8$, and $P(y = 3) = 0.2$, and the probabilities converge to 1/3 as no prioritization is specified.

The effect of the priority vector λ is discussed for $\lim_{\gamma \to \infty} \Psi(\gamma)$ such that $\lambda_i^\alpha = q_i^\alpha = P(y = \alpha | z = i)$, which is also the setting used in [2] and [6]. The state-dependent priority vectors control the vehicles in a way such that the constraints due to other traffic participants or the road geometry are met, as it is done for controlled Markov chains; see, e.g., [8].

To break down the effects of the priority vector λ, two different aspects are considered. One of them is the characteristic probability distribution m in the absence of constraints, such that $m_i^\alpha = \lambda_i^\alpha$, which is modeled as independent of the state ($m_i^\alpha = m_j^\alpha \forall i, j$). However, not all inputs meet the constraints (are drivable), such that the event C of constraint satisfaction is introduced. Due to the uncertain modeling of traffic situations, the event of constraint satisfaction C is subject to probability and stored in the constraint vector $c_i^\alpha := P(C | z = i, y = \alpha)$. As at least the constraints have to be met, the probability vector c_i^α serves as an upper bound for the priority vector λ, i.e.,

$$\lambda_i^\beta = \begin{cases} m_i^\beta, & \text{if } m_i^\beta \le c_i^\beta \\ c_i^\beta, & \text{otherwise.} \end{cases} \to m_i^{\beta-1} := m_i^{\beta-1} + m_i^\beta - c_i^\beta \cdot$$

In other words, m_i^β is cut off at c_i^β, and the cutoff probability is added to the next lower acceleration interval (see Fig. 10). This is motivated by the fact that for the considered situations of vehicle and road following (Sections V-C and D), drivers have to accelerate less or brake stronger to fulfill the safety constraints.

C. Interaction of Traffic Participants

In this section, the computation of the constraint vector $c_i^\alpha = P(C | z = i, y = \alpha)$ with respect to the interaction of two vehicles driving on the same lane is presented. The state and the input of the following vehicle A are denoted as z^A and y^A and analogously as z^B and y^B for the leading vehicle B. The constraint for this scenario is that the probability of the following vehicle crashing into the leading vehicle has to be less than ϵ, which is typically very low. Therefore, it is first checked if a certain initial situation results in a crash. As the probability distribution of vehicles is approximate (in contrast to the reachable set), the check for a crash under initial states and inputs chosen from the cells belonging to z^A, y^A, z^B, and

y^B is also approximately done for a single sample of possible initial states and inputs, i.e.,

$$x^A(0) = \texttt{center}\left(X_i^A\right), \qquad x^B(0) = \texttt{center}\left(X_j^B\right)$$

$$u^A(0) = \texttt{center}\left(U^{A^\alpha}\right), \qquad u^B(0) = \texttt{center}\left(U^{B^\beta}\right)$$

where `center` returns the volumetric center of a set. The single simulation run that approximately checks for a crash is performed as follows.

1) Simulate both vehicles for the time $\Delta t = \nu \cdot T$, $\nu \in \mathbb{N}^+$, starting from $x^A(0)$, $x^B(0)$ under the effect of u^A, u^B.
2) Simulate a sudden brake beginning at $t = \nu \cdot T$ of the leading and following vehicle until the following vehicle has stopped at $t = t_S$.
3) Check if the following vehicle has crashed into the leading vehicle for $t \in [0, t_S]$.

Events such as $z^A = i$ are abbreviated by index notation as $(z^A = i) \hat{=} z_i^A$ in the following to obtain a concise notation. The outcome of the simulation determines the conditional probability for satisfying the constraint that a crash occurs with probability less than ϵ, which is motivated by driver inattentiveness, i.e.,

$$P\left(C | z_i^A, z_j^B, y^{A^\alpha}, y^{B^\beta}, \Delta t = \nu \cdot T\right)$$

$$= \begin{cases} 1, & \text{no crash simulated} \\ \epsilon, & \text{otherwise.} \end{cases}$$

The conditional probabilities $P(C | z_i^A, z_j^B, y^{A^\alpha}, y^{B^\beta}, \Delta t = \nu \cdot T)$ can be obtained for different intervals $\Delta t = \nu \cdot T$ of constant acceleration. Long-time intervals Δt model the behavior of the foresighted drivers, who adjust their acceleration early to the changes of other drivers. More sporty drivers change their acceleration in shorter time intervals Δt. The probability distribution for time intervals in which the acceleration interval is unchanged $P(\Delta t = \nu \cdot T)$ allows the computation of

$$P\left(C | z_i^A, z_j^B, y^{A^\alpha}, y^{B^\beta}\right)$$

$$= \sum_\nu P\left(C | z_i^A, z_j^B, y^{A^\alpha}, y^{B^\beta}, \Delta t = \nu \cdot T\right) \cdot P(\Delta t = \nu \cdot T).$$

Note that the probability $P(\Delta t = \nu \cdot T)$ is not obtained online by observation of other drivers, but set according to an average distribution of all the drivers. The conditional probabilities $P(C | z_i^A, z_j^B, y^{A^\alpha}, y^{B^\beta})$ are computed offline and stored in a $(c \times c)$ array of $(d \times d)$ matrices $\Theta_{ji}^{\alpha\beta}$, where c and d are the numbers of discrete inputs and states. Using the values in $\Theta_{ji}^{\alpha\beta}$, the constraint vector for vehicle interaction is computed online as in the following proposition.

Proposition 2: Under the assumption that $P(z_i^A, y^{A^\alpha})$ and $P(z_j^B, y^{B^\beta})$ are independent, one obtains

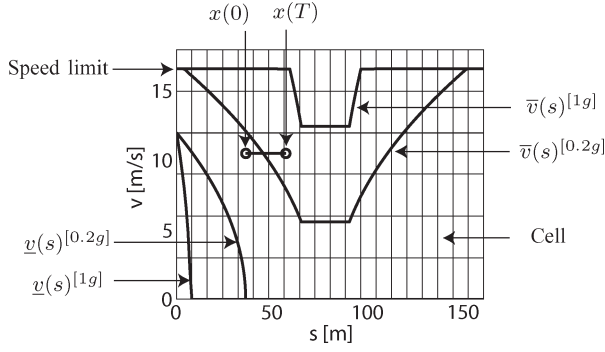$$c_i^\alpha = \sum_{j, \beta} \Theta_{ji}^{\alpha\beta} p_j^{B^\beta}.$$

Fig. 11.   Velocity profiles for two straights connected by a 90° curve (15.5-m radius) and a speed limit of $v^{\max} = 16.7$ m/s$\hat{=}60$ km/h.

Proof: After defining the events $A = (z_i^A, y^{A^\alpha})$ and $B_j^\beta = (z_j^B, y^{B^\beta})$, one can write

$$P(C, A) = \sum_{j, \beta} P\left(C | A, B_j^\beta\right) P\left(A, B_j^\beta\right)$$

$$\overset{\text{independence}}{=} \sum_{j, \beta} P\left(C | A, B_j^\beta\right) P(A) P\left(B_j^\beta\right)$$

$$\rightarrow c_i^\alpha = P(C | A) = \frac{P(C, A)}{P(A)}$$

$$= \sum_{j, \beta} P\left(C | A, B_j^\beta\right) P\left(B_j^\beta\right)$$

$$= \sum_{j, \beta} \Theta_{ji}^{\alpha\beta} p_j^{B^\beta}.$$

∎

It is clear that the independence assumption only approximates the joint probability $P(A, B_j^\beta) \approx P(A) P(B_j^\beta)$; however, this assumption simplifies the computation and has produced reasonable results for numerical examples. In traffic situations with more than two vehicles on a lane, each vehicle is only interacting with the next nearest vehicle driving in front, such that the proposed algorithm is simply applied for each vehicle that follows another vehicle.

D. Behavior Restriction Due to Road Geometry and Speed Limits

In addition to interaction with other vehicles, possible acceleration inputs are restricted due to speed limit and the road geometry in combination with the limited tire friction. For these restrictions, the velocity profile resulting from the minimum and maximum possible acceleration with respect to (2) is introduced and denoted as $\underline{v}(s)$ and $\overline{v}(s)$, respectively. An additional labeling with brackets indicates the maximum absolute acceleration, e.g., $\overline{v}(s)^{[0.5g]}$ is the fastest possible velocity profile for $a^{\max} = 0.5\,g$, and g is the gravity constant. Exemplary velocity profiles with a speed limit (possibly greater than the official speed limit to account for sporty drivers) are shown in Fig. 11.

The velocity profiles allow to compute the constraint vector $c_i^\alpha = P(C | z = i, y = \alpha)$ with respect to road geometry and

speed limit, where the event C holds when the velocity is within the velocity profile bounds ($\underline{v}(s) \leq v \leq \overline{v}(s)$). Analogous to vehicle interaction, the compliance of a constraint for state $z = i$, input $y = \alpha$, and given velocity bounds $\underline{v}(s)$ and $\overline{v}(s)$ is approximately checked by a single simulation run.

1) Simulate the vehicle for the time interval $\Delta t = T$, starting from $x(0) = \texttt{center}(X_i)$ under the effect of $u = \texttt{center}(U^\alpha)$.
2) Check whether the velocity is within the minimum and maximum velocity profile after one time increment T (see also Fig. 11), i.e.,

$$\underline{v}\left(s(T)\right)^{\left[a_d^{\max}\right]} \leq v(T) \leq \overline{v}\left(s(T)\right)^{\left[a_d^{\max}\right]}. \qquad (8)$$

The constraint vector for road geometry and speed limit is then obtained as

$$P\left(C | z_i, y^\alpha, a < a_d^{\max}\right) = \begin{cases} 1, & \text{if (8) holds} \\ 0, & \text{otherwise.} \end{cases}$$

In contrast to vehicle interaction, the constant ϵ for inattentiveness is not applied here, as the physical constraint is either met or not. After introducing the probability distribution for applied accelerations $P(a < a_d^{\max})$ among all drivers, where $0 < a_d^{\max} \leq \bar{a}^{\max}$, and $\bar{a}^{\max}$ is the physically possible acceleration, the constraint vector is

$$c_i^\alpha = P(C | z_i, y^\alpha)$$
$$= \sum_d P\left(C | z_i, y^\alpha, a < a_d^{\max}\right) P\left(a < a_d^{\max}\right).$$

It remains to combine the constraint vectors for vehicle interaction and road geometry/speed limit, which are denoted as $c_i^{\text{int},\alpha}$ and $c_i^{\text{road},\alpha}$, respectively. As it is sufficient that the most restrictive constraint is active, the total constraint is computed as

$$c_i^\alpha = \min\left(c_i^{\text{int},\alpha}, c_i^{\text{road},\alpha}\right).$$

E. Stochastic Reachable Set of the Ego Car

In contrast to other traffic participants, the trajectory of the ego car is known since the trajectory planner module is connected to the safety verification module (see Fig. 1). This means that for time points t_k, the position and the velocity are known up to a certain inaccuracy Λ of the vehicle controller for trajectory tracking such that $x(t) \in \hat{x}(t) + \Lambda$, where $\hat{x}(t)$ is the planned trajectory, and the addition is performed as a Minkowski sum.[2] For time intervals $t \in [t_k, t_{k+1}]$, the reachable set is given by the 2-D interval

$$R\left([t_k, t_{k+1}]\right) = \bigcup_{t \in [t_k, t_{k+1}]} \hat{x}(t) + \Lambda.$$

---

[2]Minkowski addition of two sets A, B: $A + B = \{a + b | a \in A, b \in B\}$.
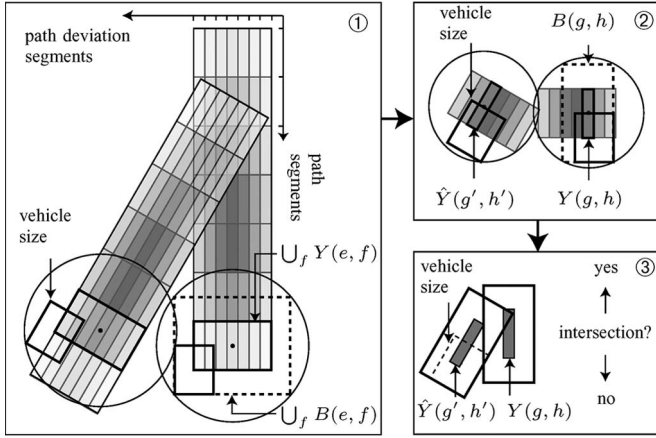
Fig. 12. Crash probability obtained from stochastic reachable sets.

The reachable set is intersected with the cells of the discretized state space, which is similar to (4), to obtain the discretized probability distribution $\hat{p}^\alpha([t_k, t_{k+1}])$ of the ego car.

VI. CRASH PROBABILITIES OF THE EGO CAR

The probabilities $p_i^\alpha([t_k, t_{k+1}])$ computed in the previous section refer to the probability that the continuous state is in a certain cell X_i under the effect of the input interval U^α. The total probability without input information is obtained by the summation

$$p_i([t_k, t_{k+1}]) = \sum_\alpha p_i^\alpha([t_k, t_{k+1}]).$$

Each state space cell i represents a position and velocity interval S_e and V_m ($e, m \in \mathbb{N}^+$ indexing position and velocity segments) such that $X_i = S_e \times V_m$, where only the probability of the position interval S_e is of interest for the computation of crash probabilities. The position probability for a path segment is obtained from the joint probabilities by summation, which results in

$$p_e^{\text{path}}([t_k, t_{k+1}]) := P(s \in S_e, t \in [t_k, t_{k+1}])$$

$$= \sum_m P(s \in S_e, v \in V_m, t \in [t_k, t_{k+1}]).$$

As the deviation probability is piecewise constant, one can also define intervals D_f in which the deviation probability is constant (see Fig. 4). Introducing the probability for a deviation segment $p_f^{\text{dev}}([t_k, t_{k+1}]) = P(\delta \in D_f, t \in [t_k, t_{k+1}])$, the probability that $s \in S_e$ and $\delta \in D_f$ is $p_{\text{ef}}^{\text{pos}} = p_e^{path} \cdot p_f^{\text{dev}}$ due to the independency assumption (see Section III). The set obtained from $s \in S_e$ and $\delta \in D_f$ is a polygon $Y(e, f)$, which is indexed by its path segment $e \in \mathbb{N}^+$ and deviation segment $f \in \mathbb{N}^+$ (see Fig. 12).

Without loss of generality, the crash probability is considered only for the ego car with one other traffic participant for simplicity in the following. In case there are more traffic participants, the following procedure has to be repeated for each one of them. For a better distinction of the variables from the other vehicle with the variables of the ego car, the variables referring to the ego car are indexed by a hat ($\hat{\square}$). To compute the crash probability, the pairs of polygons $(Y(g, h), \hat{Y}(g', h'))$ for which the vehicle bodies intersect have to be determined. Thereto, the possible set of vehicle bodies $B(g, h)$ for a set of vehicle centers in a polygon $Y(g, h)$ is introduced, which is the union of car bodies whose centers are within $Y(g, h)$ and whose orientation is equal to the direction of the path segment g (see Fig. 12). To efficiently compute the polygon pairs $(Y(g, h), \hat{Y}(g', h'))$ resulting in intersecting vehicle bodies $(B(g, h) \cap \hat{B}(g', h') \neq \emptyset)$, three steps are suggested allowing to efficiently discard nonintersecting pairs.

1) First, it is checked if the vehicle bodies $\bigcup_f B(e, f)$ of a certain path segment e can possibly intersect the vehicle bodies belonging to a path segment g of the ego car. Thereto, it is checked if the circles enclosing the set of vehicle bodies intersect, where circles are chosen since checking for their intersection is computationally cheap.
2) Next, the set of vehicle bodies $B(g, h)$, $\hat{B}(g', h')$ belonging to pairs of path segments passing the first test are again checked for intersection by the same procedure using enclosing circles.
3) Finally, the polygon pairs passing the two previous tests are directly checked for intersection. However, polytope intersection is computationally expensive, such that lookup tables are generated in advance, which contain relative positions and angles for which polygons intersect. There are different lookup tables depending on checking the intersection with a bicycle/bike, a car, or a truck.

The sets of combinations of path and deviation segments resulting in a crash are stored in a list Ω. The crash probability is obtained by adding the probabilities for the pairs of path and deviation segments in Ω as

$$p^{\text{crash}} = \sum_{(g,h,e,f) \in \Omega} \hat{p}_{gh}^{\text{pos}} \cdot p_{ef}^{\text{pos}}.$$

Note that the probability of a crash is computed in an overapproximated way, as the sets of vehicle bodies $B(g, h)$ are overapproximations due to the union of possible vehicle bodies within the uncertain vehicle center $Y(g, h)$.

VII. NUMERICAL EXAMPLES

The presented methods for the safety verification of planned paths of autonomous cars are demonstrated for two traffic situations. For both examples, the same discretization of the state and input space is used for all vehicles. The position is discretized into 40 segments of 5-m length, and the velocity is discretized into ten segments, each of which represents an interval of 2.2 m/s. Each vehicle is subject to five input intervals, and the time increment of the Markov chains is chosen as $T = 0.5$ s. The γ value for the input dynamics has been chosen as $\gamma = 0.2$, and the values of the characteristic input probability distribution are chosen as $m^{1,\dots,5} = [0.01 \quad 0.04 \quad 0.5 \quad 0.4 \quad 0.05]$.

In the first example, it is checked if the ego car can safely overtake a bicycle before reaching a T-intersection, where another car is approaching. The stochastic reachable sets of the traffic participants are given in Fig. 13. Dark regions indicate
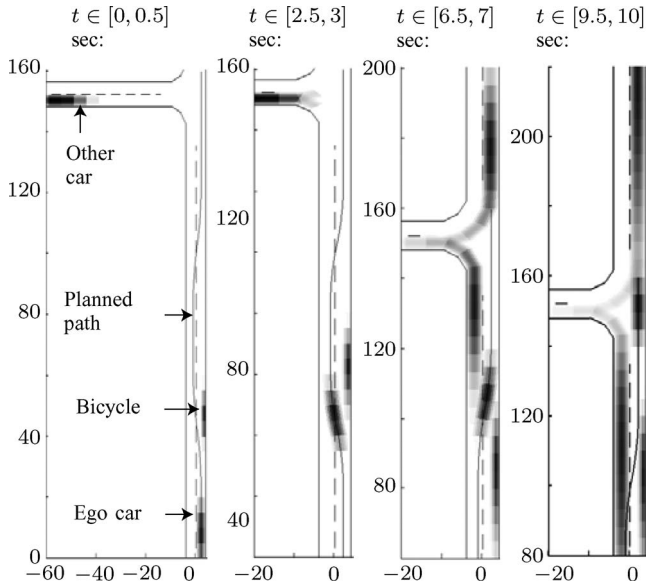
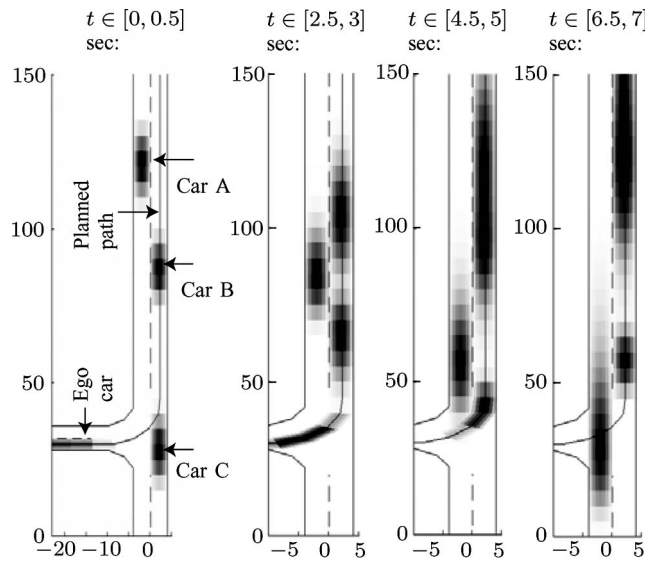Fig. 13.   Stochastic reachable sets for the overtaking scenario.

Fig. 14.   Stochastic reachable sets for the merging scenario.

high probability, whereas bright regions represent areas of low probability. To improve the visualization, the colors are separately normalized for each vehicle, i.e., the highest probability value of a vehicle is plotted in black. Note that both options (the left and right turns) are considered with probability one each for the other car. The second example shows a situation where the ego car plans to merge into another road. It is checked if it hits the oncoming cars A, B and C (see Fig. 14). The stochastic reachable sets also show the interaction between car B and C, as car C is forced to brake due to the higher velocity compared with car B. The crash probabilities for both examples are found in Fig. 15.

The examples are implemented in C++[3] and are computed on a 3.7-GHz single-core desktop computer for which the

----

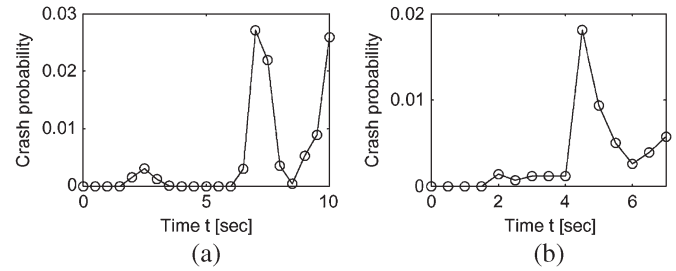[3]For convenience, the plots have been created in Matlab.

Fig. 15.   Crash probabilities of the overtaking and merging scenario. (a) Overtaking scenario. (b) Merging scenario.

TABLE I
COMPUTATIONAL TIMES OF THE NUMERICAL EXAMPLES

Discre- tization	Overtaking scenario		Merging scenario	
	Total time [sec]	Replanning time [sec]	Total time [sec]	Replanning time [sec]
High	0.56 (η : 17.9)	0.127	1.31 (η : 5.30)	0.074
Low	0.28 (η : 35.7)	0.086	0.51 (η : 13.7)	0.053
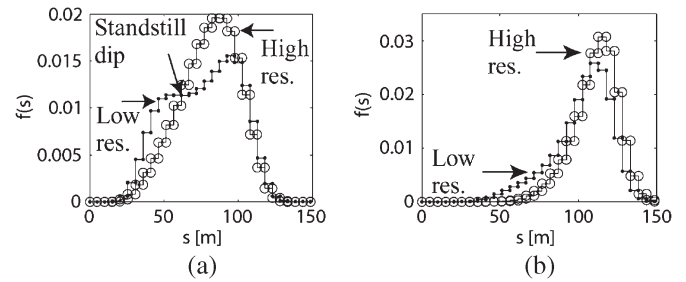
Fig. 16.   Comparison of stochastic reachable sets with low/high discretization resolution. (a) Low initial velocity $v(0) \in [4, 6]$. (b) High initial velocity $v(0) \in [12, 14]$.

computation times are listed in Table I. The $\eta = t_f/t_c$ values, where t_f is the time horizon and t_c is the computation time, state how much faster the computation is than real time. In addition to the discretization of the state and input space used so far, a coarser discretization with six instead of ten velocity intervals and three, instead of five, input intervals is computed. The computation times for the more coarse discretization are also shown in Table I. The difference in accuracy for the high- and low-resolution discretizations is tried so that it can be familiarized with a scenario where a vehicle is driving on a straight and free road. The probability distribution for the high- and low-resolution model is shown in Fig. 16. By showing the results for different initial velocities, it is shown that the accuracy of the coarser discretization significantly depends on the given situation. The bigger difference in the probability distributions for the low initial velocities is due to the fact that the vehicle is more likely to reach a standstill as the probability for the input interval representing full braking increased after the mapping from five to three discrete inputs.

Another aspect, which is considered in Table I, is the necessary time for the computation of crash probabilities if the trajectory planner forwards a replanned trajectory of the ego car while the initial situation of the other vehicles in traffic is

unchanged. This time is referred to as replanning time in Table I and does not account for the time that the planner module requires to plan the path of the ego car. The obtained times are for the case that the velocity of the ego car has been decreased by 20%.

VIII. CONCLUSION

The presented approach has allowed assessment of the safety of planned trajectories of autonomous cars by predicting the traffic situation. Uncertainties originating from measurements of other traffic participants and their unknown intentions are considered in a stochastic way. To improve the prediction accuracy, the interaction of traffic participants is included. The resulting crash probabilities of a planned path are conservative, i.e., if the crash probability is zero, then it can be guaranteed that the ego car will not cause a crash if the traffic participants stay within the predefined physical bounds, such as the maximum tire friction.

It has been shown that the approach is scalable and can be applied online. If not much computational power is available, then the discretization resolution can easily be adapted. Further, as most of the computations are based on matrix multiplications, a specialized hardware (e.g., graphics chips) could provide a low-cost solution for this approach. This would allow the use of the proposed safety-assessment algorithm for driver-assistance systems by substituting the planned path of the autonomous car with a predicted path of the human driver.

REFERENCES

[1] M. Abdel-Aty and A. Pande, "ATMS implementation system for identifying traffic conditions leading to potential crashes," *IEEE Trans. Intell. Transp. Syst.*, vol. 7, no. 1, pp. 78–91, Mar. 2006.
[2] M. Althoff, O. Stursberg, and M. Buss, "Online verification of cognitive car decisions," in *Proc. IEEE Intell. Veh. Symp.*, 2007, pp. 728–733.
[3] M. Althoff, O. Stursberg, and M. Buss, "Reachability analysis of linear systems with uncertain parameters and inputs," in *Proc. 46th IEEE Conf. Decision Control*, 2007, pp. 726–732.
[4] M. Althoff, O. Stursberg, and M. Buss, "Safety assessment of autonomous cars using verification techniques," in *Proc. Amer. Control Conf.*, 2007, pp. 4154–4159.
[5] M. Althoff, O. Stursberg, and M. Buss, "Reachability analysis of nonlinear systems with uncertain parameters using conservative linearization," in *Proc. 47th IEEE Conf. Decision Control*, 2008, pp. 4042–4048.
[6] M. Althoff, O. Stursberg, and M. Buss, "Stochastic reachable sets of interacting traffic participants," in *Proc. IEEE Intell. Veh. Symp.*, 2008, pp. 1086–1092.
[7] M. Althoff, O. Stursberg, and M. Buss, "Verification of uncertain embedded systems by computing reachable sets based on zonotopes," in *Proc. 17th IFAC World Congr.*, 2008, pp. 5125–5130.
[8] A. Arapostathis, R. Kumar, and S.-P. Hsu, "Control of Markov chains with safety bounds," *IEEE Trans. Autom. Sci. Eng.*, vol. 2, no. 4, pp. 333–343, Oct. 2005.
[9] E. Asarin, T. Dang, G. Frehse, A. Girard, C. Le Guernic, and O. Maler, "Recent progress in continuous and hybrid reachability analysis," in *Proc. IEEE Conf. Comput.-Aided Control Syst. Des.*, 2006, pp. 1582–1587.
[10] A. Barth and U. Franke, "Where will the oncoming vehicle be the next second?" in *Proc. IEEE Intell. Veh. Symp.*, 2008, pp. 1068–1073.
[11] A. E. Broadhurst, S. Baker, and T. Kanade, "A prediction and planning framework for road safety analysis, obstacle avoidance and driver information," in *Proc. 11th World Congr. Intell. Transp. Syst.*, Oct. 2004.
[12] A. E. Broadhurst, S. Baker, and T. Kanade, "Monte Carlo road safety reasoning," in *Proc. IEEE Intell. Veh. Symp.*, 2005, pp. 319–324.
[13] I. Dagli and D. Reichardt, "Motivation-based approach to behavior prediction," in *Proc. IEEE Intell. Veh. Symp.*, 2002, pp. 227–233.
[14] A. Eidehall and L. Petersson, "Statistical threat assessment for general road scenes using Monte Carlo sampling," *IEEE Trans. Intell. Transp. Syst.*, vol. 9, no. 1, pp. 137–147, Mar. 2008.
[15] J. Hillenbrand, A. M. Spieker, and K. Kroschel, "A multilevel collision mitigation approach—Its situation assessment, decision making, and performance tradeoffs," *IEEE Trans. Intell. Transp. Syst.*, vol. 7, no. 4, pp. 528–540, Dec. 2006.
[16] J. Hu, M. Prandini, and S. Sastry, "Aircraft conflict detection in presence of a spatially correlated wind field," *IEEE Trans. Intell. Transp. Syst.*, vol. 6, no. 3, pp. 326–340, Sep. 2005.
[17] W. Hu, X. Xiao, Z. Fu, D. Xie, T. Tan, and S. Maybank, "A system for learning statistical motion patterns," *IEEE Trans. Pattern Anal. Mach. Intell.*, vol. 28, no. 9, pp. 1450–1464, Sep. 2006.
[18] X. Koutsoukos and D. Riley, "Computational methods for reachability analysis of stochastic hybrid systems," in *Hybrid Systems: Computation and Control*. Berlin, Germany: Springer-Verlag, 2006, pp. 377–391.
[19] G. Lafferriere, G. J. Pappas, and S. Yovine, "A new class of decidable hybrid systems," in *Hybrid Systems: Computation and Control*, vol. 1569. Berlin, Germany: Springer-Verlag, 1999, pp. 137–151.
[20] K. Lee and H. Peng, "Evaluation of automotive forward collision warning and collision avoidance algorithms," *Veh. Syst. Dyn.*, vol. 43, no. 10, pp. 735–751, Oct. 2005.
[21] C.-F. Lin, A. G. Ulsoy, and D. J. LeBlanc, "Vehicle dynamics and external disturbance estimation for vehicle path prediction," *IEEE Trans. Control Syst. Technol.*, vol. 8, no. 3, pp. 508–518, May 2000.
[22] J. Lunze and B. Nixdorf, "Representation of hybrid systems by means of stochastic automata," *Math. Comput. Model. Dyn. Syst.*, vol. 7, no. 4, pp. 383–422, Dec. 2001.
[23] J. Lunze and J. Schröder, "Sensor and actuator fault diagnosis of systems with discrete inputs and outputs," *IEEE Trans. Syst., Man, Cybern. B, Cybern.*, vol. 34, no. 2, pp. 1096–1107, Apr. 2004.
[24] J. Maroto, E. Delso, J. Félez, and J. M. Cabanellas, "Real-time traffic simulation with a microscopic model," *IEEE Trans. Intell. Transp. Syst.*, vol. 7, no. 4, pp. 513–527, Dec. 2006.
[25] A. Polychronopoulos, M. Tsogas, A. J. Amditis, and L. Andreone, "Sensor fusion for predicting vehicles' path for collision avoidance systems," *IEEE Trans. Intell. Transp. Syst.*, vol. 8, no. 3, pp. 549–562, Sep. 2007.
[26] F. Rohrmüller, M. Althoff, D. Wollherr, and M. Buss, "Probabilistic mapping of dynamic obstacles using Markov chains for replanning in dynamic environments," in *Proc. IEEE/RSJ Int. Conf. Intell. Robots Syst.*, 2008, pp. 2504–2510.
[27] C. Schmidt, F. Oechsle, and W. Branz, "Research on trajectory planning in emergency situations with multiple objects," in *Proc. IEEE Intell. Transp. Syst. Conf.*, 2006, pp. 988–992.
[28] J. Schröder, *Modelling, State Observation and Diagnosis of Quantised Systems*. Berlin, Germany: Springer-Verlag, 2003.
[29] C. Stiller, G. Farber, and S. Kammel, "Cooperative cognitive automobiles," in *Proc. IEEE Intell. Veh. Symp.*, 2007, pp. 215–220.
[30] N. Sumpter and A. J. Bulpitt, "Learning spatio-temporal patterns for predicting object behaviour," *Image Vis. Comput.*, vol. 18, no. 9, pp. 679–704, Jun. 2000.
[31] J. van den Berg, "Path planning in dynamic environments," Ph.D. dissertation, Utrecht Univ., Utrecht, The Netherlands, 2007.
[32] E. Velenis and P. Tsiotras, "Optimal velocity profile generation for given acceleration limits: Theoretical analysis," in *Proc. Amer. Control Conf.*, 2005, pp. 1478–1483.
[33] Y. U. Yim and S.-Y. Oh, "Modeling of vehicle dynamics from real vehicle measurements using a neural network with two-stage hybrid learning for accurate long-term prediction," *IEEE Trans. Veh. Technol.*, vol. 53, no. 4, pp. 1076–1084, Jul. 2004.

Matthias Althoff received the Diploma Engineering degree in mechanical engineering in 2005 from the Technische Universität München, München, Germany, where he is currently working toward the Ph.D. degree with the Institute of Automatic Control Engineering, Faculty of Electrical Engineering and Information Technology.

His research interests include (stochastic) reachability analysis of continuous and hybrid systems and safety analysis of driving strategies of autonomous cars.

Olaf Stursberg (M'06) received the M.S. degree in chemical engineering and the Ph.D. degree from the University of Dortmund, Durtmund, Germany, in 1996 and 2000, respectively.

He was a Postdoctoral Researcher with the Department of Electrical and Computer, Carnegie Mellon University, Pittsburgh, PA, from 2001 to 2002 and a Senior Researcher with the University of Dortmund from 2003 to 2006. From 2006 to 2009, he was an Associate Professor with the Department of Electrical Engineering and Information Technology, Technische Universität München, München, Germany. Since April 2009, he has been a Full Professor with the University of Kassel, Kassel, Germany, where he heads the Institute of Control and System Theory. His main research interests include the control, optimization, and analysis of nonlinear, hybrid, and discrete event systems. Special focus is on modeling, optimal control, and formal verification of distributed automotive systems.

Martin Buss (M'95) received the Diploma Engineer degree in electrical engineering from the Technical University Darmstadt, Darnstadt, Germany, in 1990, the Doctor of Engineering degree in electrical engineering from the University of Tokyo, Tokyo, Japan, in 1994, and the Habilitation degree from the Technische Universität München, München, Germany, in 2000.

In 1988, he was a research student for one year with the Science University of Tokyo. From 1994 to 1995, he was a Postdoctoral Researcher with the Department of Systems Engineering, Australian National University, Canberra, Australia. From 1995 to 2000, he was a Senior Research Assistant and a Lecturer with the Institute of Automatic Control Engineering, Department of Electrical Engineering and Information Technology, Technische Universität München. From 2000 to 2003, he was a Full Professor, the Head of the Control Systems Group, and the Deputy Director of the Institute of Energy and Automation Technology, Faculty IV, Electrical Engineering and Computer Science, Technical University Berlin, Berlin, Germany. Since 2003, he has been a Full Professor (Chair) with the Institute of Automatic Control Engineering, Faculty of Electrical Engineering and Information Technology, Technische Universität München, where he has been with the Medical Faculty since 2008. Since 2006, he has also been the coordinator of the Deutsche Forschungsgemeinschaft Excellence Research Cluster "Cognition for Technical Systems" with CoTeSys. His research interests include automatic control, mechatronics, multimodal human–system interfaces, optimization, nonlinear, and hybrid discrete-continuous systems.